Dynamical behavior of a free-electron laser operating with a prebunched electron beam

G. Dattoli, L. Giannessi, P. L. Ottaviani,* and A. Torre
Comitato Nazionale per la Ricerca e per lo Sviluppo dell'Energia Nucleare e delle Energie Alternative, Dipartimento Innovazione, Settore Elettroottica e Laser, Centro Ricerche Energia Frascati, Casella Postale 65, 00044 Frascati, Rome, Italy
(Received 2 February 1994)

A prebunched electron beam can be exploited to reduce the rise time of a free-electron laser (FEL) oscillator, or to provide the start-up signal for an amplifier. We discuss the dynamical behavior of FEL's operating with prebunched electron beams, and analyze different regimes of operation, from low signal up to saturation. We also include short pulses effects, discussing the modifications occurring in the FEL pulse propagation equation and analyzing the relevant small signal dynamics.

PACS number(s): 41.60.Cr, 41.85.Lc, 52.75.Ms, 07.77.+p

I. INTRODUCTION

The dynamical features of a free-electron laser (FEL) operating with a suitably prebunched electron beam have been recently discussed [1,2] and it has also been stressed that a prebunched electron beam may be a unique tool to provide the start up of a FEL amplifier in regions of the spectrum where coherent seed sources are not available [3–5]. FEL oscillators too may benefit from a prebunched operation and in fact the rise time of the laser signal, namely, the time necessary to reach the saturation, may be significantly reduced without affecting the final saturated power. Very roughly speaking, the beam prebunching provides an additional gain, which, under specific conditions, may give a contribution comparable to or even larger than, the intrinsic gain of the system. We analyze the dynamical behavior of a FEL oscillator operating with a prebunched electron beam and discuss under which conditions the harmonic content of the beam may provide coherent contributions to the signal start up. The treatment will be extended to the amplifier case and to FEL operating with short pulses. This last problem will be studied discussing the modifications occurring in the FEL pulse propagation equations when the prebunching corrections are included. In particular, we consider the modifications occurring in the so-called supermode (SM) dynamics [6]. The paper is organized as follows. In Sec. II, we analyze the small signal behavior of a prebunched FEL oscillator, saturation is included using a simplified model whose correctness is then checked by means of an accurate numerical analysis. Section III contains some considerations on the dynamical behavior of a "seedless" FEL amplifier (SFELA). The modified FEL pulse propagation equations including prebunching are discussed in Sec. IV, where we also analyze the small signal behavior of the laser pulses. Section V is finally devoted to concluding remarks. In Appendix A we consider the prebunched FEL dynamics and induced electron beam energy spread and show that the numerical results can be reproduced by simple equations. Appendix B is devoted to the high gain corrections. Finally in Appendix C we discuss a simple perturbative analysis of the Liouville equation ruling the evolution of the longitudinal phase-space evolution of an electron beam undergoing a FEL interaction.

II. PREBUNCHED FEL OSCILLATOR DYNAMICS

The dynamics of a FEL operating in the long bunch condition, namely, in the case in which slippage effects can be neglected, is governed by the pendulum equation [7],

$$\frac{d^2\zeta}{d\tau^2}=|a|\cos(\zeta+\phi)\ ,\qquad \frac{d}{d\tau}a=-2\pi g_0\langle e^{-i\zeta}\rangle_{\zeta_0}\ . \tag{2.1}$$

The electron relative phase with respect to the radiation field is denoted by $\zeta(\tau)$, $|a|$ and ϕ are the amplitude and phase of the dimensionless optical field, g_0 is the small signal gain coefficient, and $\langle\ \rangle_{\zeta_0}$ represents an average over the electron initial phase ζ_0. (For further insight the reader is addressed to Ref. [7].)

Equation (2.1) holds either in small and strong signal regime. Useful information can be, however, inferred considering its small signal limit, which is obtained expanding all the relevant quantities up to the first order in the amplitude a. According to Ref. [8], the equation governing the evolution of the optical field in the small signal regime is

$$\frac{d}{d\tau}a=-2\pi g_0 b_1 e^{-i\nu_0\tau}+i\pi g_0\int_0^\tau d\xi\,\xi e^{-i\nu_0\xi}a(\tau-\xi)+i\pi g_0 b_2 e^{-2i\nu_0\tau}\int_0^\tau d\xi\,\xi a^*(\tau-\xi)e^{i\nu_0\xi}\ . \tag{2.2}$$

We have implicitly assumed that the electron beam contains an initial phase distribution

*Also at ENEA, Dipartimento Innovazione, Settore Elettroottica e Laser, Centro Ricerche Energia E. Clementel, Bologna, Italy.

$$f(\zeta_0)=\sum_{n=-\infty}^{+\infty} b_n e^{i\nu\zeta_0}, \quad b_0=1 \tag{2.3a}$$

and, thus,

$$\langle e^{-i\zeta_0}\rangle_{\zeta_0}=\frac{1}{2\pi}\int_0^{2\pi} d\zeta_0 f(\zeta_0)e^{-i\zeta_0}=b_1 ,$$
$$\langle e^{-2i\zeta_0}\rangle_{\zeta_0}=\frac{1}{2\pi}\int_0^{2\pi} d\zeta_0 f(\zeta_0)e^{-2i\zeta_0}=b_2 . \tag{2.3b}$$

Equation (2.2) has been carefully treated in Ref. [8]. It has, in fact, been shown to reduce to a third order ordinary differential equation of the type

$$\dddot{a}(\tau)+2i\nu_0\ddot{a}(\tau)-\nu_0^2\dot{a}(\tau)=i\pi g_0\{a(\tau)+b_2 a^*(\tau)e^{-2i\nu_0\tau}\} , \tag{2.4a}$$

where the dots denote derivatives with respect to τ. The initial conditions of (2.4a) are specified by

$$a(0)=a_0, \quad \dot{a}(0)=-2\pi g_0 b_1, \quad \ddot{a}(0)=2\pi i\nu_0 g_0 b_1 . \tag{2.4b}$$

The possibility of a seedless operation is due to the fact that a nonzero b_1 coefficient ensures initially nonvanishing first and second derivatives. An exact solution of Eq. (2.4a) can be obtained if the contribution due to the coefficient b_2 can be neglected. However, just to see what happens during the early stages of the interaction, we write the solution in terms of the Taylor expansion

$$a(\tau)=\sum_{n=0}^{\infty}\frac{a^{(n)}(0)}{n!}\tau^n , \tag{2.5}$$

where the superscript (n) indicates the nth derivative. At the initial times the various $a^{(n)}(0)(n\geq 3)$ are provided by the recursive relation

$$a^{(n)}(0)=-2i\nu_0 a^{(n-1)}(0)+\nu_0^2 a^{(n-2)}(0) -i\pi g_0\left[a^{(n-3)}(0)+\sum_{m=0}^{n-3}\binom{n-3}{m}(-2i\nu_0)^m \times[a^{(n-3-m)}(0)]^*\right] . \tag{2.6a}$$

In particular, for initially vanishing field, we find

$$a^{(3)}(0)=2\pi g_0\nu_0^2 b_1 ,$$
$$a^{(4)}(0)=-2\pi i g_0[\nu_0^3 b_1+\pi g_0(b_1+b_1^* b_2)] . \tag{2.6b}$$

It is, therefore, clear that the terms containing b_2 start playing a role at relatively large times and that the emission process is dominated and driven by the b_1 coefficient.

Equation (2.2) is an integrodifferential equation which can be solved using a naive series expansion and, the lowest order term of such an expansion, yields

$$a(\tau)\simeq a_0\left[1+\pi g_0\frac{2(1-e^{-i\nu_0\tau})-\nu_0\tau(e^{-i\nu_0\tau}+1)}{\nu_0^3}\right] -2\pi g_0 b_1\left[\frac{\sin(\nu_0\tau/2)}{\nu_0/2}\right]e^{-i\nu_0\tau/2} +\frac{\pi g_0 b_2}{\nu_0^3}a_0^*\left\{[\nu_0\tau-\sin(\nu_0\tau)]\sin(\nu_0\tau) -i\frac{\sin(2\nu_0\tau)-2(\nu_0\tau)\cos(\nu_0\tau)}{2}\right\} . \tag{2.7}$$

The above result can be viewed as the low gain evolution of the optical field and contains three distinct contributions.

(1) The term proportional to a_0 displays the usual behavior and leads to the well known gains equation. (The part multiplaying g_0 yields, at $\tau=1$, the complex gain function.)

(2) The term proportional to b_1 provides the coherent spontaneous emission.

(3) The last term is proportional to b_2 and, therefore, describes the part of the field evolution due to the second order bunching coefficient.

It is now worth mentioning an interesting point. If we define the gain in the usual way

$$G=\frac{|a(1)|^2-|a(0)|^2}{|a(0)|^2} , \tag{2.8}$$

and neglect the g_0^2 contributions, we end up with

$$G\simeq -\pi g_0\frac{\partial}{\partial\nu_0}\left[\frac{\sin(\nu_0/2)}{\nu_0/2}\right]^2 -4\pi g_0\frac{|b_1|}{|a_0|}\left[\frac{\sin(\nu_0/2)}{\nu_0/2}\right]\cos(\nu_0-\chi) +\frac{2\pi g_0 b_2}{\nu_0^3}\{\cos\chi_1(\nu_0-\sin\nu_0)\sin\nu_0 +\tfrac{1}{2}\sin\chi_1[\sin(2\nu_0)-2\nu_0\cos\nu_0]\} ,$$
$$\chi=\arg(a_0^* b_1), \quad \chi_1=\arg\left[\frac{a_0^*}{a_0}b_2\right] . \tag{2.9}$$

The first term is the usual antisymmetric FEL gain. The last two contributions, improperly called gain terms since they depend on the initial field amplitude a_0, may help the signal growth according to whether the χ phases are properly adjusted. Although in an amplifier experiment the phases are randomly distributed and, thus, the new contributions average to zero, in an oscillator configuration the field coherently rearranges the phases in such a way that after each round trip the bunching dependent terms may positively interfere. Such a conjecture may be verified using a rather trivial oscillator mod-

el. Denoting with n the index of the round trip we assume that the oscillator evolution can be reproduced by the rate equation

$$a_{n+1}=\{a_n[1+\pi g_0 A(\nu)]-2\pi g_0 b_1 B(\nu) + \pi g_0 b_2 a_n^* C(\nu)\}\sqrt{1-\eta} \ . \tag{2.10}$$

The ν functions A,B,C are those appearing in Eq. (2.7) at $\tau=1$ and η denotes the cavity losses.

Equation (2.10) accounts for the small signal and low gain evolution of the intracavity optical field. Preliminary, albeit not fully correct information, can be obtained transforming (2.10) into an ordinary differential equation. Neglecting the b_2 term (such an assumption will be justified below) we get

$$\frac{d}{dn}a=[(1-\xi)\pi g_0 A(\nu)-\xi]a - 2\pi g_0 b_1(1-\xi)B(\nu) \quad (\xi=1-\sqrt{1-\eta}) \ , \tag{2.11a}$$

assuming that a is initially vanishing, we get

$$a(n)=-2\pi g_0 b_1(1-\xi)B(\nu)\frac{e^{[(1-\xi)\pi g_0 A(\nu)-\xi]n}-1}{(1-\xi)\pi g_0 A(\nu)-\xi} \ . \tag{2.11b}$$

It is, therefore, clear that one can associate to the b_1 contribution an equivalent seed intensity. More quantitative considerations can be developed if we note that the square modulus of the dimensionless amplitude a is linked to the FEL saturation intensity

$$[I_S \ (\mathrm{MW/cm^2})]=6.9\times 10^2\left[\frac{\gamma}{N}\right]^4\frac{1}{\{[\lambda_u \ (\mathrm{cm})]Kf_B(\xi)\}^2} \tag{2.12}$$

by the relation

$$|a|^2=0.8\pi^4\left[\frac{I}{I_S}\right] , \tag{2.13}$$

where γ is the electron-beam relativistic factor, N is the number of undulator periods, λ_u is the undulator period length, K is the undulator parameter, and $f_B(\xi)=J_0(\xi)-J_1(\xi)$ is the Bessel-factor correction, where $\xi=\frac{1}{4}K^2/(1+K^2/2)$. In terms of these, the small signal gain coefficient is $g_0=(8\pi N^3/\gamma^3)\{[\lambda_u K f_B(\xi)]^2/\Sigma_E\}I/I_A$, where Σ_E is the electron-beam cross section and $I_A\cong 17\,000$ A is the Alfvén current. According to Eq. (2.11a) the contribution of the coherent spontaneous emission is

$$[I_{\mathrm{CS}} \ (\mathrm{MW/cm^2})]\simeq\frac{5}{n^2}g_0^2|b_1|^2[I_S \ (\mathrm{MW/cm^2})] \ , \tag{2.14a}$$

and since

$$\tfrac{1}{2}g_0[I_S \ (\mathrm{MW/cm^2})]=\frac{1}{4N}[P_E \ (\mathrm{MW/cm^2})] \ , \quad [P_E \ (\mathrm{MW/cm^2})]=[E \ (\mathrm{MeV})J \ (\mathrm{A/cm^2})] \ , \tag{2.14b}$$

we can write ($g_0|b_1|^2\ll 1$)

$$[I_{\mathrm{CS}} \ (\mathrm{MW/cm^2})]=\mu[P_E \ (\mathrm{MW/cm^2})] \ , \quad \mu=\frac{g_0|b_1|^2}{4N} \ , \tag{2.14c}$$

and μ defines a kind of efficiency of the one pass coherent spontaneous emission process. Let us now go back to Eq. (2.11), and write it in practical units so that the evolution of the field intensity can be cast in the form ($\xi\ll 1$)

$$I(n)\simeq\frac{5}{\pi^4}|b_1|^2\left|\frac{B(\nu)}{A(\nu)}\right|^2 e^{2[(1-\xi)\pi g_0 \mathrm{Re}\,A(\nu)-\xi]n}I_S \ . \tag{2.15a}$$

We have assumed n large enough that the -1 contribution on the right-hand side of (2.11b) can be neglected. According to Eq. (2.15a) the seed equivalent term for the field evolution is

$$I_0\simeq\frac{5}{\pi^4}|b_1|^2\left|\frac{B(\nu)}{A(\nu)}\right|^2 I_S \ , \tag{2.15b}$$

evaluating the ν dependent functions at $\nu=2.6$ and neglecting the losses we find

$$I_0\simeq 1.54|b_1|^2 I_S \ , \tag{2.15c}$$

and it is interesting to note that I_0 is independent from the electron-beam current. A modest bunching coefficient, of the order of few percent, may provide an input I_0 which is a relatively large number (of the order of $10^{-3}I_S$), the rise time of the oscillator can be, therefore, significantly reduced. In particular, assuming that the onset of saturation is reached for $I(n^*)=I_S$ we find from (2.15) (n^* is the number of round trips corresponding to the rise time)

$$n^*\simeq-\frac{\ln[1.54|b_1|^2]}{\alpha} \ , \tag{2.16}$$

where α is the net gain of the system. Oscillators operating with a not prebunched electron beam have a typical rise time with n^* specified by

$$\alpha n^*\simeq 21 \ . \tag{2.17}$$

The prebunching reduces, therefore, the rise time of a factor $-\ln[1.54|b_1|^2]/21$. Assuming, e.g., $|b_1|\simeq 3.5\times 10^{-2}$, we find that the rise time is reduced by a factor of 3.

The small signal dynamics of a low gain prebunched FEL oscillator is shown in Fig. 1, describing the round trip evolution of the intracavity optical field intensity. The figure indicates that the rate equation (2.10) and the analytical solution of its differential reduction [see Eq. (2.11b)] provides almost identical results. The discrepancy derives from the last term in Eq. (2.10) containing the b_2 coefficient and neglected in Eq. (2.11a). The corrections due to the second order bunching becomes appreciable at large round trip numbers, when the field is large enough that saturation effects are significant. The contributions due to b_2 are therefore canceled by saturation. Equation (2.11b) may be, therefore, considered fully reliable for the description of the small signal regime dynamics.

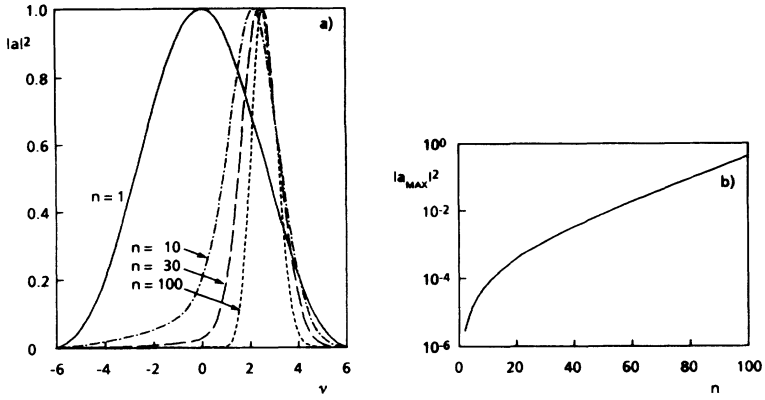

FIG. 1. (a) $|a|^2$ vs ν at different round trips. (b) $|a_{\max}|^2$ vs the round trip number.

Saturation can be easily included, using the semianalytical model of Ref. [9]. The intracavity power growth can be reproduced using the rate equation (n denotes the round trip number)

$$x_{n+1}=(1-\eta)[G(x_n)+1]x_n \ , \tag{2.18}$$

where

$$x=I/I_S \ , \qquad G(x)=G_{\max}\frac{1-e^{-\beta x}}{\beta x}, \quad \beta=\frac{\pi}{2}1.0145 \ , \tag{2.19}$$

the input value of the iteration is $x_0=1.54|b_1|^2$. The validity of the model has been tested in the case of a not prebunched operation and Figs. 2 and 3 confirm its validity for the prebunched case too. The physical information contained in Fig. 2 are worth stressing.

(a) The first few round trips are dominated by the coherent spontaneous emission.

(b) When the field is large enough the evolution becomes predicted by the small signal theory.

(c) The seed intensity I_0 [see Eq. (2.15c)] is obtained extrapolating the linear behavior.

(d) The induced electron-beam energy spread reflects the optical field dynamical behavior. In correspondence of I_0, namely, extrapolating the linear behavior of σ_ε^i vs n, a $\sigma_{\varepsilon,0}^i$ can be introduced. Such a value can be

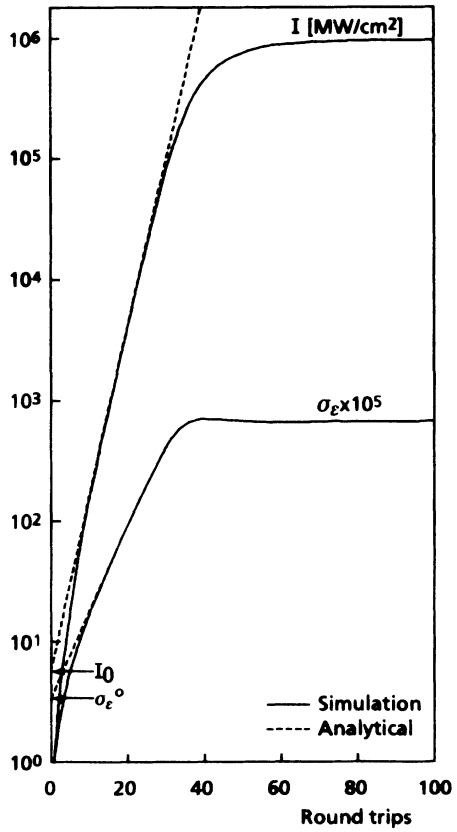

FIG. 2. Prebunched FEL dynamics. (I) — — — Small signal approximation (analytical result); —— numerical results including saturation; $\sigma_\varepsilon \equiv$ induced energy spread (numerical); $b_1=-2.79\times10^{-3}$, $\gamma=420.7$; $N=40$; $g_0\simeq0.5462$; $I_S=3.08\times10^6$ MW/cm^2; $G\simeq0.513$.

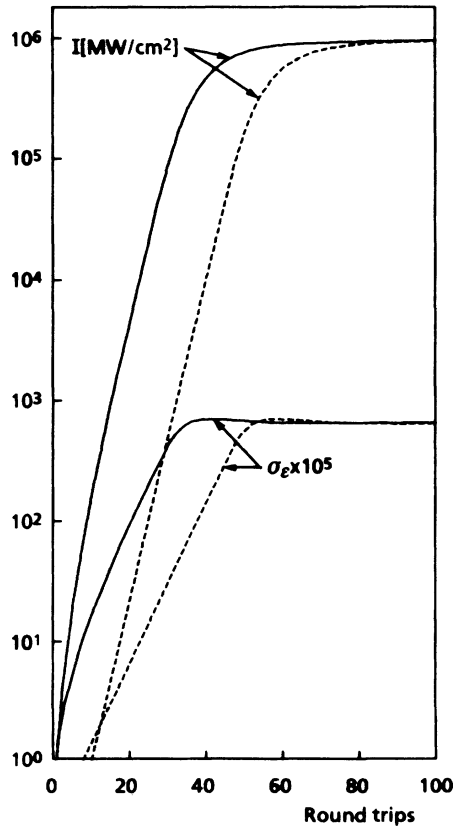

FIG. 3. FEL intracavity dynamics: — — — prebunched case (same parameters as Fig. 2); —— nonprebunched case input seed $I_0=10^{-7}I_S$.

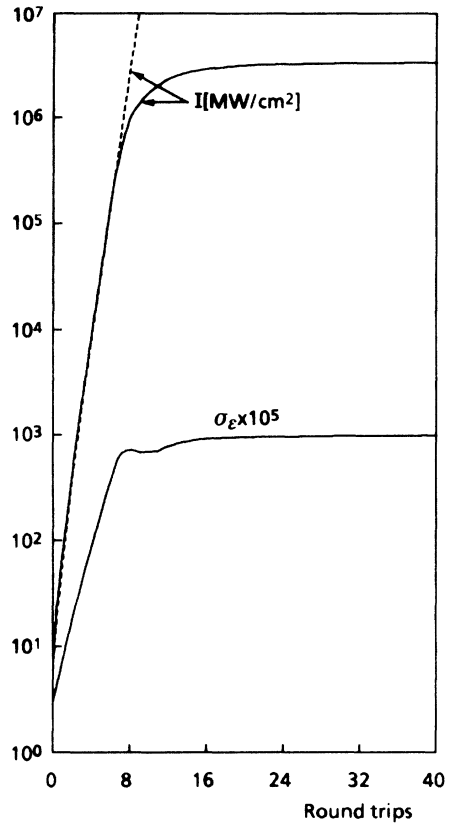

FIG. 4. Same as Fig. 2. $g_0=2.728$; $I_S=2.36\times10^5$ MW/cm^2.

quantified as (see Appendix A)

$$\sigma^i_{\varepsilon,0}\simeq\frac{0.678}{N}|b_1|\ , \tag{2.20}$$

which is in agreement with the results of the simulation (see Fig. 2). The comparison between prebunched and conventional operations indicates that the predicted reduction of rise times may be considered reliable.

As already remarked the analysis developed so far does not include high gain corrections which becomes important when $g_0>0.5$. Figure 4 shows that the low gain approximation leading to Eq. (2.7) is reasonably good even for large values of g_0.

Further comments are given in Appendix B.

III. SELF-AMPLIFICATION OF PREBUNCHING

In the previous section we discussed the dynamical behavior of a FEL oscillator operating with a prebunched electron beam. We have seen that one of the most significant effects is a reduction of the rise time of the optical signal, since the bunching coefficient provides a kind of equivalent input seed.

Also in the case of a FEL amplifier the start up "seed" is linked to the bunching coefficient and a preliminary idea of the prebunched FEL amplifier is obtained solving Eq. (2.2) at the resonance ($\nu_0=0$).

In this case, the solution can be obtained in the form of a series

$$a(\tau)=\sum_n a_n(\tau)\ , \tag{3.1a}$$

where

$$\begin{aligned}
&a_0(\tau)=-2\pi g_0 b_1\tau,\quad a_1=2i(\pi g_0)^2(b_1+b_1^* b_2)\frac{\tau^4}{4!}\ ,\\
&a_{2n+1}=2(i)^{2n+1}(\pi g_0)^{2n+2}(b_1+b_1^* b_2)\\
&\qquad\times(1-|b_1|^2)^{2n-2}\frac{\tau^{3n+4}}{(3n+4)!}\ ,\\
&a_{2n}=2(-1)^n(\pi g_0)^{2n+1}b_1(1-|b_2|^2)^n\frac{\tau^{6n+1}}{(6n+1)!}\ .
\end{aligned} \tag{3.1b}$$

The above series is very fast convergent and confirms the rather unimportant role played by the coefficient b_2 (Fig. 5). Neglecting b_2 Eq. (2.2) (at $\nu_0=0$) can be solved in closed form, namely [8],

$$\begin{aligned}
a=\frac{2ib_1(\pi g_0)^{2/3}}{3}\{&e^{-i(\pi g_0)^{1/3}\tau}+e^{i\pi/3}e^{1/2(\sqrt{3}+i)(\pi g_0)^{1/3}\tau}\\
&+e^{i\pi/3}e^{-1/2(\sqrt{3}+i)(\pi g_0)^{1/3}\tau}\}\ .
\end{aligned} \tag{3.2}$$

A comparison between solutions (3.2) and (3.1) is given in Fig. 6. For $g_0=100$, five terms in the series (3.1a) are sufficient to reproduce the exact solution, when g_0 takes larger values further terms should be taken into account.

Equation (3.2) is rather interesting from the physical point of view. The field evolution is indeed dominated by the exponential having the argument with positive real part. The square modulus can be, therefore, approximated as [$\tau=Z/(\lambda_u N)$]

$$\begin{aligned}
&|a|^2\simeq\frac{4|b_1|^2(\pi g_0)^{4/3}}{9}e^{4\sqrt{3}\rho Z/(N\lambda_u)}\ ,\\
&\rho=\frac{1}{4\pi}\left[\frac{\pi g_0}{N^3}\right]^{1/3}\ ,
\end{aligned} \tag{3.3a}$$

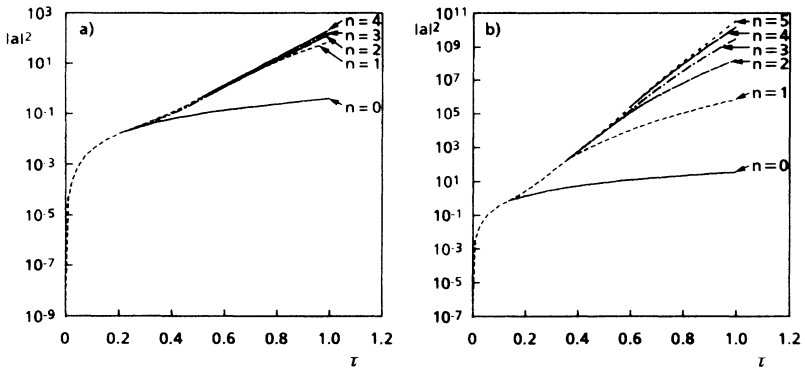

FIG. 5. (a) $|a|^2$ vs τ solution (3.1a) and various order of approximation ($g_0=100$, $b_1=10^{-3}$; $b_2=10^{-3}$). (b) ($g_0=1000$, $b_1=10^{-3}$; $b_2=10^{-3}$).

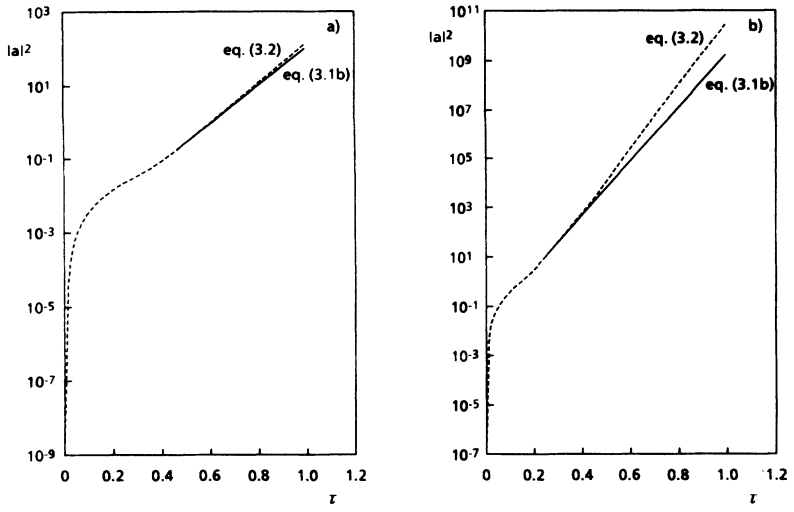

FIG. 6. Comparison between solutions (3.1b) (including the first five terms) and (3.2) (a) ($g_0=100$, $b_1=10^{-3}$; $b_2=10^{-3}$). (b) ($g_0=1000$, $b_1=10^{-3}$; $b_2=10^{-3}$).

where Z is the longitudinal coordinate along the undulator direction.

Using Eqs. (2.12)–(2.14) we can write (3.3a) in practical units, i.e.,

$$[I\ (\mathrm{MW/cm^2})]\simeq\tfrac{1}{9}|b_1|^2\rho[P_E\ (\mathrm{MW/cm^2})]e^{4\sqrt{3}\rho Z/(N\lambda_u)}\ . \tag{3.3b}$$

In this case, the seed equivalent intensity is provided by

$$[I_0\ (\mathrm{MW/cm^2})]=|b_1|^2\rho[P_E\ (\mathrm{MW/cm^2})]\ . \tag{3.4}$$

Recalling that ρ is the efficiency of a high gain FEL amplifier with constant parameter and that $\rho[P_E\ (\mathrm{MW/cm^2})]$ is the power density at the saturation, we can conclude that

$$[I_0\ (\mathrm{MW/cm^2})]=|b_1|^2[I_{\mathrm{sat}}\ (\mathrm{MW/cm^2})] \tag{3.5}$$

and that the saturation length is linked to the bunching coefficient by

$$Z_S\simeq\frac{\lambda_u}{2\sqrt{3}\rho}\ln\left[\frac{3}{|b_1|}\right]\ . \tag{3.6}$$

The general behavior of the signal growth in the high gain regime is characterized by a first part, which is essentially quadratic. In this region, the evolution is dominated by the coherent spontaneous emission term, a_0 in Eq. (3.1b). To understand the extension of this region, we keep the first two terms of the series (3.1a) and write

$$a(\tau)\simeq-2(\pi g_0)\left[b_1\tau+i(\pi g_0)(b_1+b_1^*b_2)\frac{\tau^4}{4!}\right]\ . \tag{3.7}$$

Neglecting the coefficient b_2 we find that in Eq. (3.7) the second term dominates on the first if

$$\tau>\left[\frac{4!}{(\pi g_0)}\right]^{1/2}\ , \tag{3.8a}$$

or, equivalently,

$$Z>0.229\frac{\lambda_u}{\rho}\ . \tag{3.8b}$$

In Fig. 7 we compare the evolution of the field for seedless and seed injected amplifiers. In the former case, the beam is assumed to be prebunched with bunching coefficient b_1, in the latter, the field evolves from an initial seed $a_0=2b_1(\pi g_0)^{2/3}$. Further comments are presented in the concluding remarks.

IV. PREBUNCHING AND PULSE PROPAGATION

The analogous of Eqs. (2.1), when short pulses effects are included, reads [7]

$$\frac{\partial}{\partial\tau}a(Z,\tau)=-2\pi g_0\sigma(Z+\Delta\tau)\langle\exp[-i\zeta(Z+\Delta\tau,\tau)]\rangle\ ,$$
$$\ddot{\zeta}=|a(Z-\Delta\tau,\tau)|\cos[\zeta(Z,\tau)+\phi(Z-\Delta\tau,\tau)]\ , \tag{4.1}$$

where $\sigma(Z)$ is the longitudinal electron-beam shape and $\Delta=N\lambda$ is the slippage length. Using the same procedure as before, we write the small signal limit of (4.1) as

$$\frac{\partial}{\partial\tau}a(Z,\tau)=-2\pi g_0b_1(Z+\Delta\tau)\sigma(Z+\Delta\tau)e^{-i\nu_0\tau}$$
$$+i\pi g_0\sigma(Z+\Delta\tau)\int_0^\tau d\tau'(\tau-\tau')a[Z+\Delta(\tau-\tau'),\tau']e^{-i\nu_0(\tau-\tau')}+i\pi g_0\sigma(Z+\Delta\tau)b_2(Z+\Delta\tau)$$
$$\times\int_0^\tau d\tau'(\tau-\tau')a^*[Z+\Delta(\tau-\tau'),\tau']e^{-i\nu_0(\tau+\tau')}\ , \tag{4.2}$$

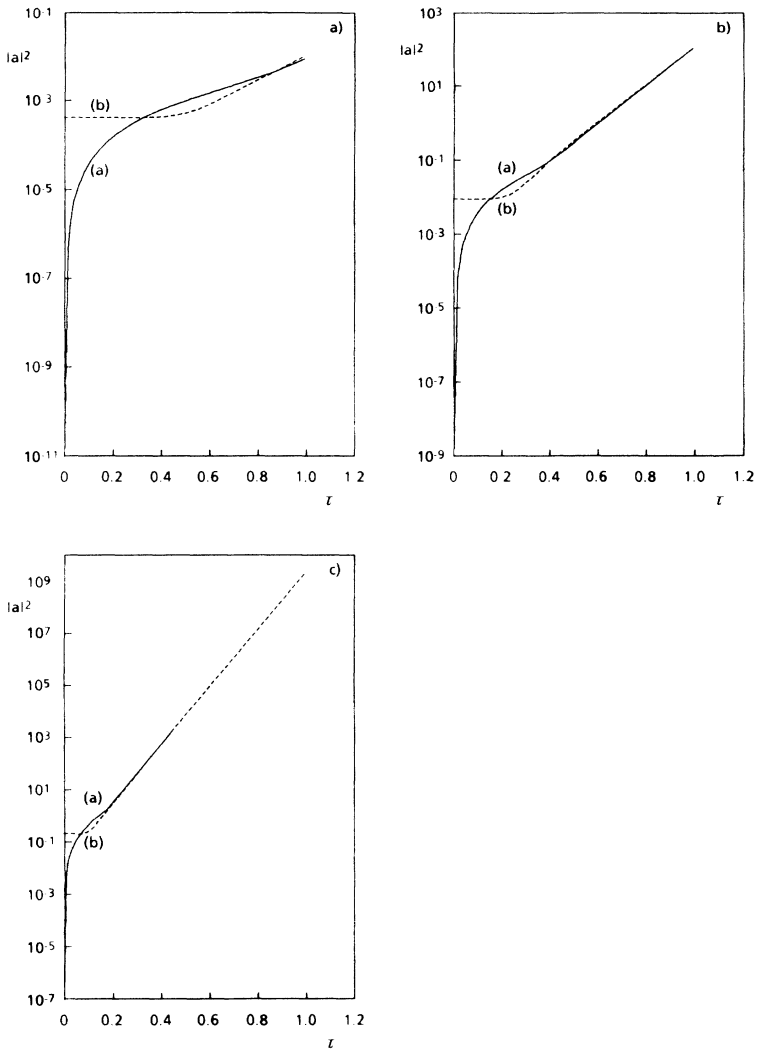

FIG. 7. Comparison between seedless (a) and seeded (b) amplification. Input seed $a_0=2b_1(\pi g_0)^{2/3}$, $b_1=10^{-2}$, (a) $g_0=10$, (b) $g_0=100$, (c) $g_0=1000$.

the bunching coefficients are, in general, functions of Z, but here, for the sake of simplicity, we will ignore such a dependence.

As we have already remarked, when the field intensity is low, the emission process is dominated by the coherent spontaneous emission. In this case, the 0th order field is a Z-dependent function which can be derived from the equation

$$\frac{\partial}{\partial\tau}a_0(Z,\tau)=-2\pi g_0\sigma(Z+\Delta\tau)b_1e^{-i\nu_0\tau}, \tag{4.3a}$$

which can be solved in a rather straightforward way. Setting indeed

$$\frac{\partial}{\partial\tau}a_0(Z,\tau)=-2\pi g_0\sigma\left[Z+i\Delta\frac{\partial}{\partial\nu_0}\right]b_1e^{-i\nu_0\tau}, \tag{4.3b}$$

we immediately find

$$a_0(Z,\tau)=-2\pi g_0\sigma\left[Z+i\Delta\frac{\partial}{\partial\nu_0}\right]\times b_1\frac{\sin(\nu_0\tau/2)}{\nu_0/2}e^{-i\nu_0\tau/2}. \tag{4.4}$$

If, furthermore, we assume that the electron-bunch shape is Gaussian,

$$\sigma(Z)=e^{-Z^2/2\sigma_Z^2}. \tag{4.5}$$

The solution (4.4) can be cast in the form

$$a_0(Z,\tau)=-2\pi g_0b_1\times\sum_{n=0}^{\infty}\frac{1}{n!}\left[\frac{-i}{\sqrt{2}}\right]^n\mu_c^nH_n\left[\frac{Z}{\sqrt{2}\sigma_Z}\right]\times e^{-Z^2/(2\sigma_Z^2)}\times\left[\frac{\partial}{\partial\nu_0}\right]^n\left[\frac{\sin(\nu_0\tau/2)}{\nu_0/2}e^{-i\nu_0\tau/2}\right], \tag{4.6}$$

where H_n denotes the nth order Hermite polynomial and

$$\mu_c=\frac{\Delta}{\sigma_Z} \tag{4.7}$$

is the coupling parameter measuring the importance of

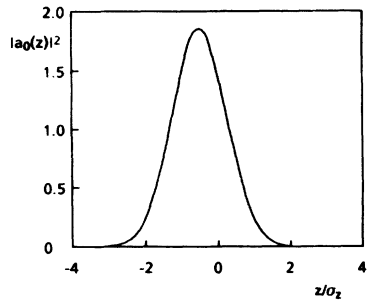

FIG. 8. Coherent spontaneous emission vs Z. $\nu_0 \simeq 0$; $g_0=1$; $b_1=1/\sqrt{2\pi}$; $\mu_c=1$.

the slippage effects. When μ_c is a small quantity, i.e., when the slippage distance is small compared to the bunch length, the field generated by the coherent spontaneous emission reproduces the electron-bunch shape (see Fig. 8). For larger μ_c values some deformation occurs owing to the contribution of higher order terms.

Neglecting the b_2 coefficient, Eq. (4.2) can be written as

$$\frac{\partial}{\partial\tau}a(Z,\tau)=-2\pi g_0 b_1\sigma(Z+\Delta\tau)e^{-i\nu_0\tau} +i\pi g_0\sigma(Z+\Delta\tau) \times\int_0^{\tau}d\xi\,\xi a(Z+\Delta\xi,\tau-\xi)e^{-i\nu_0\xi}\,, \tag{4.8}$$

and its small signal limit can be obtained setting

$$a(Z+\Delta\xi,\tau-\xi)\simeq a(Z+\Delta\xi,\tau)\,. \tag{4.9}$$

With this assumption Eq. (4.8) can be cast in the integral form

$$a(Z,\tau)=a(Z,0)-2\pi g_0 b_1\int_0^{\tau}\sigma(Z+\Delta\tau')e^{-i\nu_0\tau'}d\tau' +i\pi g_0\int_0^{\tau}\sigma(Z+\Delta\tau')e^{-i\nu_0\tau'}d\tau' \times\int_0^{\tau'}a(Z+\Delta\xi,\tau)\xi e^{-i\nu_0\xi}d\xi\,, \tag{4.10a}$$

rearranging the limits of integration in the last part of (4.10a) we find

$$a(Z,\tau)-a(Z,0)=i\pi g_0\int_0^{\tau}d\tau''a(Z+\Delta\tau'',\tau)e^{-i\nu_0\tau''} \times\int_{\tau''}^{\tau}d\tau'\sigma(Z+\Delta\tau') -2\pi g_0 b_1\int_0^{\tau}\sigma(Z+\Delta\tau')e^{-i\nu_0\tau'}d\tau'\,. \tag{4.10b}$$

Finally setting

$$Z+\Delta\tau'=\tilde{Z}\,,\qquad \Delta\tau''=\chi\,, \tag{4.11}$$

we end up with

$$a(Z,\tau)=a(Z,0)-2\pi\frac{g_0}{\Delta}b_1\int_0^{\Delta\tau}\sigma(Z+\chi)e^{-i(\nu_0/\Delta)\chi}d\chi +i\pi\frac{g_0}{\Delta^3}\int_0^{\Delta\tau}d\chi\,a(Z+\chi,\tau)\chi e^{-i\nu_0\chi/\Delta} \times\int_{Z+\chi}^{Z+\Delta\tau}d\tilde{Z}\,\sigma(\tilde{Z})\,. \tag{4.12}$$

Equation (4.12) can be exploited to derive the round trip evolution for a FEL oscillator operating with short pulses in the low gain small signal regime. Taking into account the fact that the cavity should be shortened by an amount δL to compensate the lethargy, we get

$$a(Z-2\delta L,n+1) =\left[a(Z,n)-\frac{2\pi g_0 b_1}{\Delta}\int_0^{\Delta}\sigma(Z+\chi)e^{-i(\nu_0/\Delta)\chi}d\chi +i\frac{\pi g_0}{\Delta^3}\int_0^{\Delta}d\chi\,a(Z+\chi,n)\chi e^{-i\nu_0(\chi/\Delta)} \times\int_{Z+\chi}^{Z+\Delta}d\tilde{Z}\sigma(\tilde{Z})\right]\sqrt{1-\eta}\,. \tag{4.13}$$

Assuming small losses, expanding $a(Z-2\delta L)$ up to the first order in δL and transforming the rate equation into a differential equation, we get

$$2T_c\frac{\partial a(Z)}{\partial t}+(\Delta g_0\theta)\frac{\partial a(Z)}{\partial Z}+\eta a(Z) =-2\frac{(2\pi)^{3/2}g_0 b_1}{\mu_c}\int_0^{\Delta}f(Z+\chi)e^{-i(\nu_0\chi/\Delta)}d\chi +\frac{i(2\pi)^{3/2}g_0}{\mu_c\Delta^2}\int_0^{\Delta}d\chi\,a(Z+\chi)\chi e^{-i\nu_0(\chi/\Delta)} \times\int_{Z+\chi}^{Z+\Delta}f(\tilde{Z})d\tilde{Z}\,, \tag{4.14}$$

where T_c is the round trip period and $t/T_c=n$,

$$f(Z)=\frac{1}{\sqrt{2n}\,\sigma_z}e^{-Z^2/\sigma_Z^2}\,,\qquad \theta=-\frac{4\delta L}{g_0\Delta}\,. \tag{4.15}$$

θ is the cavity detuning parameter, where σ_Z is the electron-beam rms bunch length, $\Delta=N\lambda_r$, and $\lambda_r=(\lambda_u/2\gamma^2)(1+K^2/2)$. Equation (4.14) is the equation defining the SM (see Refs. [6,9]) plus a source term due to the electron-beam prebunching, Eq. (4.14) can be recast in the more convenient form

$$\frac{\partial}{\partial\bar{\tau}}a(Z,\bar{\tau})=\hat{B}f(Z)+\hat{K}a(Z,\bar{\tau})\,, \tag{4.16}$$

where

$$\hat{B}=-2i\frac{(2\pi)^{3/2}}{\mu_c}\int_0^{\Delta}e^{-i(\chi/\Delta)\hat{\nu}_0}d\chi\ ,$$

$$\hat{K}=\left\{i\frac{(2\pi)^{3/2}}{\mu_c\Delta^2}\int_0^{\Delta}d\chi\ \chi[-e^{-i(\chi/\Delta)\hat{\nu}_0}F(Z)+F(Z+\Delta)e^{-i(\chi/\Delta)\hat{\nu}_0}]-(\Delta\theta)\frac{\partial}{\partial Z}-\frac{\eta}{g_0}\right\}, \tag{4.17}$$

$$\hat{\nu}_0=\nu_0+i\Delta\frac{\partial}{\partial Z},\quad \bar{\tau}=\tfrac{1}{2}g_0\frac{t}{T_c}\ ,$$

and $F(Z)$ is the primitive of $f(Z)$. It has already been shown that SM's are eigenfunctions of the operator $\hat{K}$ and that they provide a biorthogonal system [6]. The source term and the field $a(Z,\bar{\tau})$ can be expanded in SM's, namely [the SM are denoted by $U_m(Z)$],

$$\hat{B}f(Z)=\sum_m C_m U_m(Z)\ ,\qquad a(Z,\bar{\tau})=\sum_m a_m(\bar{\tau})U_m(Z)\ , \tag{4.17a}$$

thus, getting for $a_m(\bar{\tau})$ the first order differential equation

$$\frac{d}{d\bar{\tau}}a_m=C_m+\lambda_m a_m\ , \tag{4.18}$$

where λ_m is the eigenvalue of the mth SM. Assuming $a_m(O)=0$ we find

$$a_m(\bar{\tau})=C_m\frac{e^{\lambda_m\bar{\tau}}-1}{\lambda_m}\ . \tag{4.19}$$

The conclusion is, therefore, analogous to those relevant to the continuous beam case. The field growth is initially driven by the coherent spontaneous emission, which can be projected on the SM basis and the evolution of each component is given by Eq. (4.19). For sufficiently large times (after the first few round trips), the field evolution can be viewed as that of an initial input amplitude, given by

$$a_0(Z)=\sum_m\frac{C_m}{\lambda_m}U_m(Z)\ . \tag{4.20}$$

The intracavity evolution of a prebunched FEL oscillator with the inclusion of pulse propagation effects is shown in Fig. 9.

The figure shows electron and optical pulses at the undulator input after each round trip. It is evident that after the first round trips the optical pulse becomes narrower and it slips behind the electron pulse because the cavity length reduction is not sufficient to compensate the lethargy.

V. CONCLUDING REMARKS

We have discussed the dynamical behavior of a FEL operating with a prebunched electron beam but we did not clarify how such a prebunching can be achieved. In the case of FEL operating at long wavelength with short pulses, the bunching mechanism may be naturally provided by the radio frequency accelerating system itself [1]. In the case of shorter wavelengths, the most efficient bunching mechanism is the FEL itself. To give a further idea on the usefulness of a prebunched FEL operation we consider the setup of Fig. 10. Two FEL oscillators are separated by a drift region. The same electron beam drives both oscillators and the second is assumed to be turned at a harmonic of the first. When the intracavity power increases in the first oscillator the electron beam undergoes energy modulation and bunching which may favor the FEL dynamics in the second oscillator. It has also been shown that the bunching coefficient of the nth harmonic is a function of the intracavity power. In the case of the third harmonic, including also the effect of a dispersive section, we find a bunching coefficient at the second undulator input given by [8]

$$|b_3|\simeq 0.2(1+\delta)^3\pi^5\left[\frac{I_1}{I_{S1}}\right]^{3/2}\ , \tag{5.1}$$

where $\delta=L_D/L_u^{(1)}$ (see Fig. 10), I_1 and $I_{S,1}$ refer to the intracavity and saturation intensities of the first oscilla-

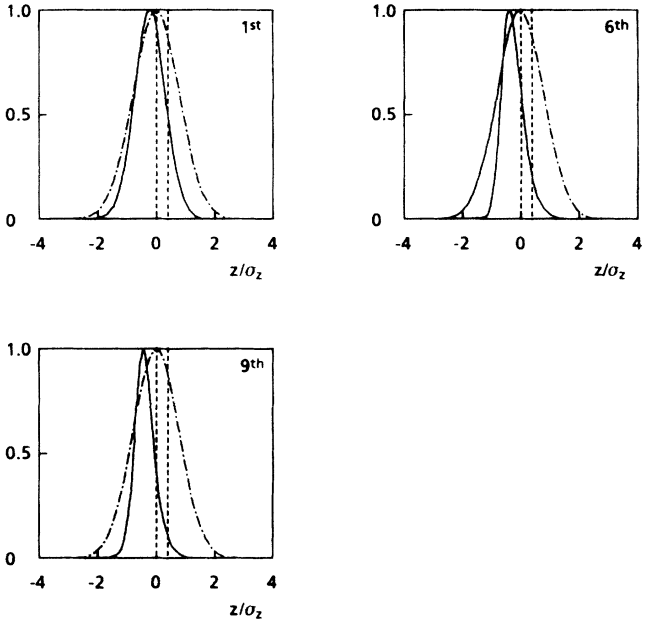

FIG. 9. Intracavity pulse evolution at different round trips ($n=1,6,9$) ($b_1=0.01$, $g_0=0.5$, $\eta=0.1$, $\mu_c=0.5$, $\theta=0.232$). The dotted line is the electron bunch profile and the continuous line represents the optical field profile.

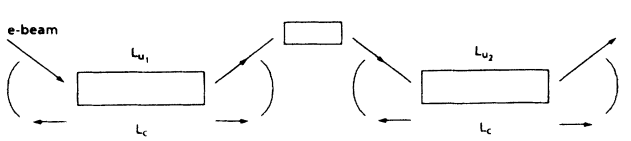

FIG. 10. Schematic layout of a tandem FEL device (e beam denotes an electron beam).

tor. According to Eq. (2.15b) the input seed of the second oscillator is proportional to the cube of the intracavity intensity of the first. This simple result gives an idea of the role played by energy modulation, bunching and energy transfer. Equation (5.1) holds far from saturation. When nonlinear effects arise the dynamical behavior of the two coupled oscillators becomes more complicated and will be discussed in a dedicated paper.

In Sec. III, we have discussed the dynamical behavior of a SFELA and we have discussed the field evolution at $\nu_0=0$. The behavior at $\nu_0\neq 0$ is not significantly different. In the high gain regime the maximum of the amplification occurs at $\nu_0\simeq 1.7$ and, for large times, can be reproduced by

$$|a|^2\simeq\frac{4|b_1|^2(\pi g_0)^{4/3}}{9}e^{4\sqrt{3}\rho Z/\lambda_u}\times\left\{1+\tfrac{1}{9}(6-\sqrt{3}\nu_0)\frac{\nu_0}{(\pi g_0)^{1/2}}\right\}. \tag{5.2}$$

A final point we want to touch is that relevant to the energy distributions. When we derived Eq. (2.2), we have averaged on the relative phases ξ_0, but not on the different electron energies. To give an idea of how energy distribution effects should be included and how these may modify Eq. (2.2), we consider the case of a prebunching induced by a FEL interaction and take into account the $b_{0,1}(\nu)$ coefficients only, which read (for the details see Appendix C)

$$\begin{aligned} b_0(\nu)&=f(\nu)\ ,\\ b_1(\nu)&=|a_0|\frac{e^{-i\nu}-1}{2\nu}\frac{\partial}{\partial\nu}f(\nu)\ , \end{aligned} \tag{5.3}$$

where a_0 is the amplitude of the field inducing the bunching and $f(\nu)$ is the energy distribution of the electron beam, which is assumed to be Gaussian and, thus,

$$\begin{aligned} f(\nu)&=\frac{1}{\sqrt{2\pi}(\pi\mu_\varepsilon)}\exp\left[-\frac{(\nu-\nu_0)^2}{2(\pi\mu_\varepsilon)^2}\right]\ ,\\ \mu_\varepsilon&=4N\sigma_\varepsilon\ , \end{aligned} \tag{5.4}$$

with σ_ε being the rms relative energy spread. According to (5.3), Eq. (2.2) should be modified as follows

$$\frac{\partial a}{\partial\tau}=-2\pi g_0 B_1(\nu_0;\mu_{\varepsilon,\tau})+i\pi g_0\int_0^\tau d\xi\,\xi e^{-i\nu_0\xi-[(\pi\mu_\varepsilon\xi)^2/2]}a(\tau-\xi) \tag{5.5}$$

and

$$B_1(\nu_0;\mu_{\varepsilon,\tau})=|a_0|\int_{-\infty}^{+\infty}\left[e^{-i\nu\tau}\frac{e^{-i\nu}-1}{2\nu}\frac{\partial}{\partial\nu}f(\nu)\right]d\nu\ . \tag{5.6}$$

If the beam is monoenergetic, $\mu_\varepsilon\to 0$ and $f(\nu)$ become a Dirac function so that

$$B_1(\nu_0;\mu_\varepsilon;\tau)=-|a_0|\left\{\frac{\partial}{\partial\nu}e^{-i\nu\tau}\frac{e^{-i\nu}-1}{2\nu}\right\}_{\nu=\nu_0}. \tag{5.7}$$

In a forthcoming note, we will present a more detailed analysis including the evaluation of higher order bunching coefficients.

APPENDIX A

One of the byproducts of the FEL interactions is the energy spread induced by the interaction itself on the electron beam. It has been shown that this quantity can be parametrized using a rather simple scaling relation [9]

$$\sigma_i(x)\simeq\frac{0.433}{N}e^{-\beta x/4}\left[\frac{\beta x}{1-e^{-\beta x}}-1\right]^{1/2}. \tag{A1}$$

As for the gain saturation, $\sigma_i(x)$ is just a function of x, which is the ratio between the intracavity and saturation intensities.

A small value of x, (A1) can be approximated by

$$\sigma_i(x)\simeq\frac{0.433}{N}\left[\frac{\beta x}{2}\right]^{1/2}. \tag{A2}$$

Using for x_0 the value predicted by Eqs. (2.15c), namely,

$$x_0\simeq 1.54|b_1|^2\ , \tag{A3}$$

we find Eq. (2.20), which can be viewed as the equivalent intrinsic energy spread of the electron beam.

APPENDIX B

We have already stressed that the coefficient b_2 scarcely affects the evolution of the optical field a. Equation (2.2) can, therefore, be written as

$$\frac{d}{d\tau}a=-2\pi g_0 b_1 e^{-i\nu_0\tau}+i\pi g_0\lambda\int_0^\tau d\xi[\xi e^{-i\nu_0\xi}a(\tau+\xi)]\ , \tag{B1}$$

where λ is a convenient expansion parameter. Equation (B1) belongs to the class of Volterra integrodifferential equations and, thus, the solution expressed as the series expansion

$$a(\tau)=\sum_n\lambda^n a_n(\tau),\quad |\lambda|<\infty \tag{B2}$$

converges for any λ value.

Here we report the first three terms of the series $(a_{0,1,2}(\tau))$ omitting the contributions containing g_0^3 corrections

$$\begin{aligned} a_0(\tau)&=a_0-2\pi g_0 b_1\left[\frac{\sin(\nu_0\tau/2)}{\nu_0/2}\right]e^{-i\nu_0\tau/2}\ ,\\ a_1(\tau)&=a_0\pi g_0\frac{2(1-e^{-i\nu_0\tau})-i\nu_0\tau(e^{-i\nu_0\tau}+1)}{\nu_0^3}\\ &\quad+b_1(\pi g_0)^2\frac{(i\nu_0^2\tau^2+4\nu_0\tau-6i)e^{-i\nu_0\tau}+6i+2\nu_0\tau}{\nu_0^4}\ ,\\ a_2(\tau)&=a_0\frac{(\pi g_0)^2}{6\nu_0^6}\{60-i24\nu_0\tau-3\nu_0^2\tau^2\\ &\quad-e^{-i\nu_0\tau}[60+i36\nu_0\tau-9\nu_0^2\tau^2-i\nu_0^3\tau^3]\}\\ &\quad+O(g_0^3)\ . \end{aligned} \tag{B3}$$

The contributions with $g_0^{n>1}$ provide the so-called high gain corrections.

APPENDIX C

The average appearing in the second of Eqs. (2.1) should be written including the energy distribution. Denoting with $\rho(\nu,\zeta)$ the electron-beam distribution in longitudinal phase space, we perform the averages according to the prescription

$$\langle\ \rangle_{\zeta,\nu}=\frac{1}{2\pi}\int_0^{2\pi}d\zeta\int_{-\infty}^{+\infty}\rho(\nu,\zeta)\ . \tag{C1}$$

The phase-space evolution of an initially unbunched electron-beam undergoing a FEL interaction is specified by the Liouville equation

$$\frac{\partial\rho}{\partial\tau}=-\nu\frac{\partial}{\partial\zeta}\rho+|a|\sin\zeta\frac{\partial\rho}{\partial\nu}\ . \tag{C2}$$

We assume that the electron beam is at the initial time a function of ν only

$$\rho(\nu,\zeta;0)=f(\nu)\ . \tag{C3}$$

We perform the low gain approximation so that $|a|$ can be kept constant during one interaction time and solve (C2) using the naive series

$$\begin{aligned}&\rho=\sum_n|a|^n\rho_n\ ,\\&\rho_n(0)=f(\nu)\delta_{n,0}\ .\end{aligned} \tag{C4}$$

Inserting (C4) in (C2) we find the recursive relations ($n>0$)

$$\frac{\partial}{\partial\tau}\rho_n=-\nu\frac{\partial}{\partial\zeta}\rho_n+\sin\zeta\frac{\partial}{\partial\nu}\rho_{n-1}\ , \tag{C5}$$

whose solution is ($n>0$)

$$\rho_n=e^{\nu\tau(\partial/\partial\zeta)}\frac{\partial}{\partial\nu}\int_0^\tau d\tau' e^{\nu\tau'(\partial/\partial\zeta)}\left[\sin\zeta\frac{\partial}{\partial\nu}\rho_{n-1}\right]\ . \tag{C6}$$

Since

$$\rho_0(\tau)=f(\nu)\ , \tag{C7}$$

we find

$$\rho_1(\tau)=\int_0^\tau d\tau'\sin[\zeta+v(\tau'-\tau)]\frac{\partial}{\partial\nu}f(\nu)\ , \tag{C8}$$

which have been derived using the identity

$$e^{a(d/dx)}f(x)=f(x+a)\ . \tag{C9}$$

Up to the lowest order in $|a|$ we find

$$\rho(\zeta,\nu;\tau)\simeq f(\nu)+|a|\frac{\cos(\zeta-\nu\tau)-\cos\zeta}{\nu}\frac{\partial}{\partial\nu}f(\nu)\ . \tag{C10}$$

The b_1 coefficient will be specified by

$$\frac{1}{2\pi}\int_0^{2\pi}\rho(\zeta,\nu;\tau)e^{-i\zeta}d\zeta=|a|\frac{e^{-i\nu\tau}-1}{2\nu}\frac{\partial}{\partial\nu}f(\nu)\ . \tag{C11}$$

[1] A. Doria, R. Bartolini, J. Feinstein, G. P. Gallerano, and R. H. Pantell, IEEE J. Quantum Electron. **QE-29**, 1428 (1993).

[2] G. Dattoli, L. Giannessi, and A. Torre, J. Opt. Soc. Am. B **10**, 2136 (1993).

[3] R. Bonifacio, L. De Salvo Sonza, P. Pierini, and E. T. Scharleman, Nucl. Instrum. Meth. **1304**, 787 (1990).

[4] R. Barbini, F. Ciocci, G. Dattoli, L. Giannessi, G. Maino, C. Mari, A. Marino, C. Ronsivalle, and A. Torre, ENEA Report No. RT/INN/90.35, 1990 (unpublished).

[5] I. Ben Zvi, F. F. Di Mauro, S. Krinsky, M. G. White, and L. H. Yu, Nucl. Instrum. Methods Phys. Res. Sect. A **296**, 737 (1990).

[6] G. Dattoli, T. Hermsen, A. Renieri, A. Torre, and J. C. Gallardo, Phys. Rev. A **37**, 4326 (1988).

[7] W. B. Colson, *Classical Theory of Free Electron Laser,* Laser Handbook, edited by W. B. Colson, C. Pellegrini, and A. Renieri (North-Holland, Amsterdam, 1990), Vol. VII.

[8] G. Dattoli and P. L. Ottaviani, J. Opt. Soc. Am. B (to be published).

[9] G. Dattoli, A. Renieri, and A. Torre, *Lectures on the Free Electron Laser Theory and Related Topics* (World Scientific, Singapore, 1993).